Assessing the two-dimensional behaviour of drystone retaining walls by full-scale experiments and yield design simulation

Anne Sophie Colas, Jean Claude Morel, Denis Garnier

HAL Id: hal-00944474
https://hal.archives-ouvertes.fr/hal-00944474

Submitted on 4 Mar 2014

Assessing the two-dimensional behaviour of drystone retaining walls by full-scale experiments and yield design simulation

A.-S. COLAS*,†, J.-C. MOREL* and D. GARNIER‡

Drystone walling is a widespread form of construction that utilises local materials. It has received growing interest over the past few years, owing to the recognition of its rich heritage in the framework of sustainable development. However, the growth of dry masonry has been slowed by the lack of scientific evidence proving its reliability. The authors have previously established a model based on yield design to assess drystone wall stability. This theoretical approach has been supplemented by field experiments on full-scale drystone retaining walls that were backfilled until failure with a cohesionless soil. These field experiments followed a first set of experiments in 2002–2003 in which the walls were loaded using hydrostatic pressure. The aim of these experimental programmes was to achieve better understanding of drystone masonry behaviour under loading, and of its failure mode. The present paper consists of a comparative analysis of these theoretical and experimental results, and provides a richer understanding of drystone retaining wall phenomenology. Further perspectives on this work are presented in the conclusion.

KEYWORDS: full-scale tests; limit state design/analysis; retaining walls; soil/structure interaction

INTRODUCTION

The term 'drystone' refers to masonry built by fitting interlocking stones together without mortar. This technique utilises local materials and knowledge to fill local building needs, yet drystone constructions can be found on five continents, and in every region where raw material is available and land development is difficult. In France, for instance, drystone constructions account for 14% of the retaining walls along the former national road network (Odent, 2000). In the UK, it is estimated that there are approximately 9000 km of dry-masonry retaining walls on the road network (O'Reilly *et al.*, 1999). The success of this technique can be attributed to its simplicity, as only a supply of stone and a few tools are required.

In the last few decades, drystone walling has received growing attention, owing to the necessity of maintenance and the repair of its rich heritage, as well as to new construction demands. The sustainable qualities of this ancient technique make it an innovative, modern-day solution. A large number of projects have been launched to protect the drystone heritage, to prove its important role in land-use planning, and to promote its use for repair or new constructions. However, the development of drystone masonry has recently been slowed by the lack of scientific knowledge regarding its reliability.

Drystone retaining structures are very difficult to model, for two main reasons. First, the masonry is strongly heterogeneous while presenting certain regularity: as a medium that is both periodic and random, drystone masonry is extremely complex to simulate. Second, when dealing with drystone retaining structures, it is necessary to take into account the backfill and the soil–structure interaction, which means that soil mech-anics must be accounted for. Simulations on drystone constructions fall into two categories: (a) macro-mechanical approaches, where the masonry is treated as a continuous medium (Arya & Gupta, 1983; Cooper, 1986; Villemus *et al.*, 2007; Mundell *et al.*, 2009); and (b) micro-mechanical approaches (finite- or distinct-element methods), where the wall is represented as a combination of blocks (Dickens & Walker, 1996; Harkness *et al.*, 2000; Powrie *et al.*, 2002; Zhang *et al.*, 2004; Claxton *et al.*, 2005). In addition, only a few recent experiments have been undertaken on drystone retaining structures (Villemus *et al.*, 2007; Mundell *et al.*, 2010).

In an attempt to model drystone retaining structures, the authors have developed a multi-scale approach based on periodic homogenisation and yield design analysis. This simulation was validated by comparisons with distinct-element simulations (Colas *et al.*, 2008) and two-dimensional scaled-down physical models (Colas *et al.*, 2010a). This study has been completed by full-scale field experiments on 2·5 m high drystone walls backfilled until failure with a cohesionless soil; the experimental protocol can be found in Colas *et al.* (2010b). The present paper presents an innovative analysis of drystone retaining walls based on these theoretical and experimental data. In this work, the original results of the field trials will be evaluated and compared with those obtained by Villemus *et al.* (2007), to highlight the characteristics of drystone wall behaviour. Finally, the two experimental programmes will be analysed using the yield design simulation previously described.

In this paper, the model and the experimental protocol will first be briefly discussed. Then the results of the experimental programmes will be analysed to reveal specific characteristics of drystone behaviour. Finally, experimental and theoretical critical heights will be compared to validate the model. Further perspectives on this work are discussed as a conclusion.

PRESENTATION OF MODEL AND EXPERIMENTAL DATA

Yield design modelling of drystone retaining walls

The simulation presented here relies on yield design (Salençon, 1990). This theory enables the evaluation of the

ultimate bearing capacity of a structure, knowing only its geometry, loading mode and yield criterion. The lower and upper ultimate load bounds are determined by an interior approach, based on statically admissible stress fields, and by an exterior approach, based on kinematically admissible virtual velocity fields. The last approach is used in this paper.

The model is briefly presented here, but calculations are detailed in Colas *et al.* (2010a). A similar yield design simulation was developed to model drystone walls loaded by hydrostatic pressure, and can be found in Colas *et al.* (2008).

Hypotheses. The simulation deals with a dry-joint earth-retaining structure treated in two dimensions, which is supported by a rock foundation of the same material as the wall blocks (Fig. 1). The geometric, loading and strength parameters are defined as follows.

(*a*) Geometry: The wall has a height h, thickness at the top l, front batter λ_1, back batter λ_2, joint inclination α, backfill height h_s and slope β (Fig. 1).
(*b*) Loading: The only loadings considered in the study are the respective unit weights, γ and γ_s, of the wall and its backfill soil respectively
(*c*) Yield criterion: Considering the drystone masonry as periodic, its yield criterion is defined by a homogenisation method for periodic media developed by de Buhan & de Felice (1997) (Fig. 2). The joints are assumed to have a purely frictional Mohr–Coulomb criterion, depending only on the block friction angle ϕ, and the stones are considered to be infinitely resistant. The yield criterion of the homogenised masonry is presented in Fig. 3. The soil is considered to be a Mohr–Coulomb material, depending on its friction angle ϕ_s.

Principle of virtual work. The kinematic approach of yield design theory is based on the principle of virtual work: the

Fig. 3. Representation of strength domain of drystone masonry (solid tint) by Colas *et al.* (2010a) deduced from the strength domain of jointed masonry (hatched tint) by de Buhan & de Felice (1997) (*m* is the slenderness ratio of the blocks and $f = \tan\phi$, with ϕ being the friction angle of the blocks)

work of the external forces, W^e, has to remain lower than the maximum resisting work, W^{mr}, for any kinematically admissible velocity field, v.

$$W^e = \int_V \gamma v \, dV + \int_S (\sigma n) v \, dS \le W^{mr} \quad (1)$$

In this study, two virtual velocity fields were used, considering the classical failure modes used for retaining structures: translation of a zone of soil and of masonry (Fig. 4(a)); and shearing of a zone of soil combined with rotation of a block of masonry (Fig. 4(b)).

The definition of these velocity fields enables one to express the work of the external forces, W^e, as a cubic polynomial in h_s, the backfill height. Considering the purely frictional criteria chosen for the masonry and the backfill, the maximum resisting work, W^{mr}, vanishes to zero. Thus equation (1) can be written

$$W^e = p_3 h_s^3 + p_2 h_s^2 + p_1 h_s + p_0 \le 0 \quad (2)$$

Ultimate backfill height. This ultimate loading height, h_s^+, is the minimum value of h_s over all virtual velocity fields, which verifies equation (2) and is the positive root of W^e; it
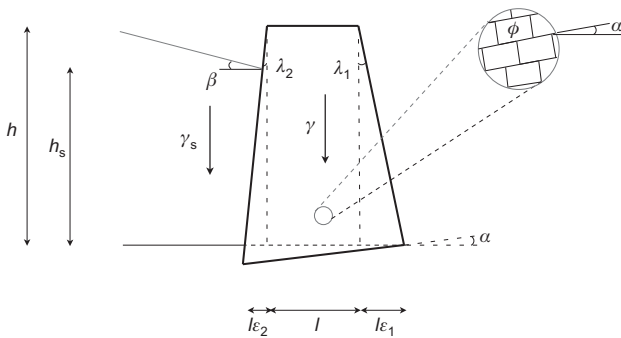

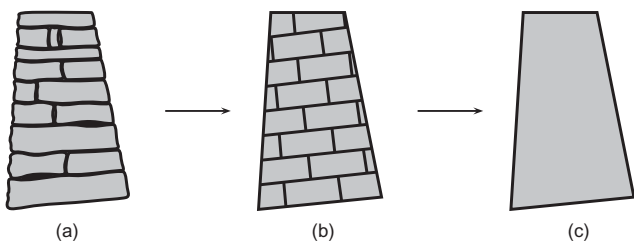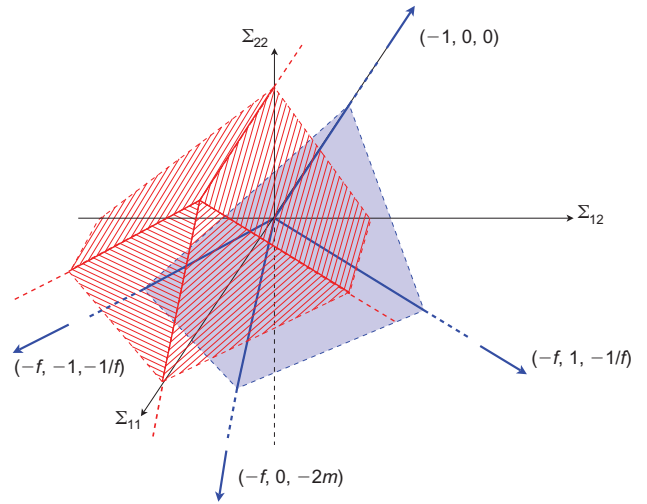Fig. 1. Drystone retaining wall modelling: hypotheses of geometry, loading and yield criterion

Fig. 2. Idealisation of drystone masonry (a), in periodic regular masonry (b) and periodic homogenisation of the regular masonry (c)
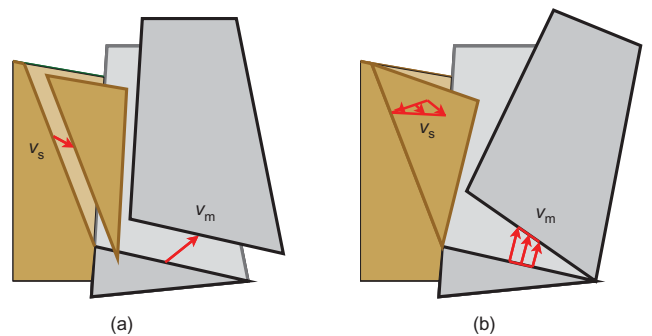

Fig. 4. (a) Translational virtual velocity fields in wall and soil; (b) rotational virtual velocity field in wall and shearing velocity field in soil

depends only on the geometry, loading and strength of the structure.

$$h_s^+ = \text{function} \left(\underbrace{h, l, \lambda_1, \lambda_2, \alpha, \beta,}_{\text{geometry}} \underbrace{\gamma, \gamma_s,}_{\text{loading}} \underbrace{\phi, \phi_s}_{\text{strength}} \right) \quad (3)$$

Full-scale field trials on drystone retaining walls

Aim of experiments. The experimental programmes undertaken in 2002–2003 (Villemus, 2004) and 2007–2008 (Colas, 2009) at the ENTPE aimed to provide a better understanding of drystone two-dimensional behaviour by way of calibration and validation simulations. Full-scale trials are essential to take into account the strong heterogeneity of drystone masonry, as well as the specificities of soil–structure interaction.

The first experimental programme (denoted 'V') was intended to focus on the drystone masonry characteristics. Thus five full-scale drystone experimental walls were constructed by professional masons, with different geometries (2–4 m high) and materials (soft limestone 'l' and schist 's') for experimentation. The walls were loaded by a hydrostatic pressure, which is fully characterised, until failure. The focus was on the general behaviour of drystone structures. Complementary information can be found in Villemus *et al.* (2007).

The second experimental programme (denoted 'C') concentrated on the effect of earth pressure on drystone walls and soil–structure interaction; the drystone masonry specifics had been studied in the previous programme. Thus four full-scale drystone walls of similar geometries (2·5 m high) and different materials (granite 'g', schist 's' and hard limestone 'L') were loaded with a cohesionless backfill until failure. The experimental protocol can be found in Colas *et al.* (2010b); the complete results of the field trial will be provided in this paper.

Characteristics of constitutive materials. The physical and geometrical characteristics of the walls and loadings were chosen considering the availability of materials on site, the feasibility of the experiment, and the results expected.

Local stones were used to respect the sustainability component of drystone construction; as a consequence, the stones used in the two experimental programmes were different. In particular, the limestone, which was soft in the first programme, was hard in the second programme. The friction angle of the stones was measured using Casagrande shear box tests (Villemus *et al.*, 2007; Colas *et al.*, 2010b). Stones

were weighed using a hydrostatic balance. The stones composing the wall were weighed after each test to determine the void percentage in drystone walls.

The backfill used in the second experimental programme was rolled gravel, which was chosen for its cohesionless characteristics and its greater pressure on the wall, compared with drift gravel. The soil characteristics were measured by triaxial tests on samples of gravel (diameter of the sample = 15 cm, height of the sample = 30 cm) reproducing on-site conditions. These tests provide a soil unit weight of $\gamma_s = 14·9$ kN/m^3 and a friction angle of $\phi_s = 37·7°$ (Colas *et al.*, 2010b).

The walls of the first experimental programme were designed using a limit equilibrium simulation developed for drystone walls (Villemus *et al.*, 2007). Different heights and profiles were tested to evaluate the influence of geometry on wall stability. In the second field trials, walls were designed using the yield design simulation presented above. We decided to keep the same height and profile for the different walls, but some modifications occurred for practical reasons (Colas *et al.*, 2010b).

The physical and geometrical characteristics of the experimental walls are summarised in Tables 1 and 2.

Experimental device. For the experiments, the self-bearing walls were loaded until failure using water discharged in a tide pool situated along the back face of the wall in the first programme (Fig. 5(a)) and rolled gravel laid along its natural slope, which was delimited by lateral formworks, in the second programme (Fig. 5(b)). The displacement of the central section of the wall was measured using nine displacement cable sensors (paths 2–10 in Fig. 6) fixed on a steel beam. The loading height was recorded by another cable sensor (path 11).

Results. The metrological equipment provided the evolution of the wall profile depending on the load. It was decided to represent the loading by the wall eccentricity – that is, the distance between the centre of the foundation, D, and a point D^* where the moment of the actions of the wall on the foundation is nil (Fig. 7) – rather than by the loading height, because this made it possible to take into account the loading height as well as the geometrical and physical characteristics of the loading material and the wall (Villemus *et al.*, 2007; Colas *et al.*, 2010b).

The first experiment with the cohesionless backfill was nullified by a technical problem: the wall displacements were so great that some blocks moved along the dimension of the wall length, and were blocked by the formworks used to

Table 1. Geometrical and physical characteristics of experimental walls loaded by hydrostatic pressure

	Wall				
	V1l	V2l	V3l	V4l	V5s
Wall height, h: m	2·00	1·95	4·00	2·00	4·25
Wall length, L: m	2·00	2·00	3·00	2·00	2·95
Wall thickness at top, l: m	0·60	0·91	1·20	0·66	1·16
Wall batter, f_1: %	15	0	15	12	15
Wall counter-slope, f_2: %	0	0	0	0	0
Joint inclination, α: degrees	0	0	0	4·0	8·5
Wall unit weight, γ: kN/m^3	15·4	14·9	15·7	15·7	18·0
Block friction angle, ϕ: degrees	36·0	36·0	36·0	36·0	28·5
Ultimate water height, h$^+$: m	1·74	1·90	3·37	1·94	3·62
Sliding	Yes	Yes	Yes	Yes	Yes
Overturning	No	Yes	No	Yes	No

Table 2. Geometrical and physical characteristics of experimental walls loaded by pulverulent backfill

	Wall			
	C1g	C2s	C3s	C4L
Wall height, h: m	2·50	2·50	2·50	2·50
Wall length, L: m	4·00	4·00	4·00	4·00
Wall thickness at top, l: m	0·45	0·45	0·55	0·50
Wall batter, f_1: %	6	6	6	6
Wall counter-slope, f_2: %	0	0	0	0
Joint inclination, α: degrees	3·4	3·4	9·1	9·1
Backfill slope, β: degrees	26·4	31·7	32·6	34·9
Wall unit weight, γ: kN/m^3	21·0	20·0	20·0	21·8
Soil unit weight γ_s: kN/m^3	14·9	14·9	14·9	14·9
Block friction angle, ϕ: degrees	27	25	25	35
Soil friction angle, f_s: degrees	37·7	37·7	37·7	37·7
Interface friction angle, δ: degrees	37·7	37·7	37·7	37·7
Ultimate backfill height, h^+: m	–	2·41	2·96	2·95
Sliding	–	Yes	No	No
Overturning	–	Yes	Yes	Yes

(a)

(b)

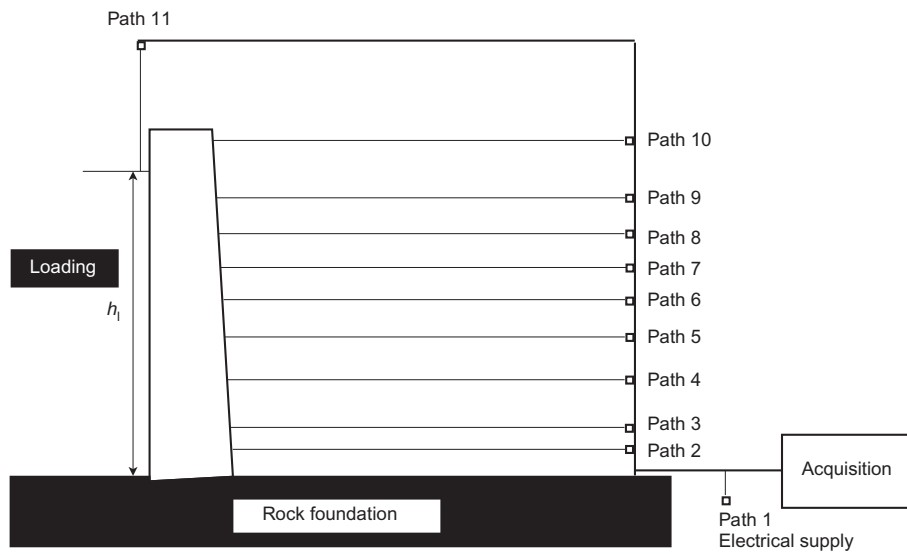**Fig. 5. (a) Hydrostatic loading process; (b) rolled gravel backfill loading process**

Fig. 6. Acquisition system during experimental programmes on drystone walls
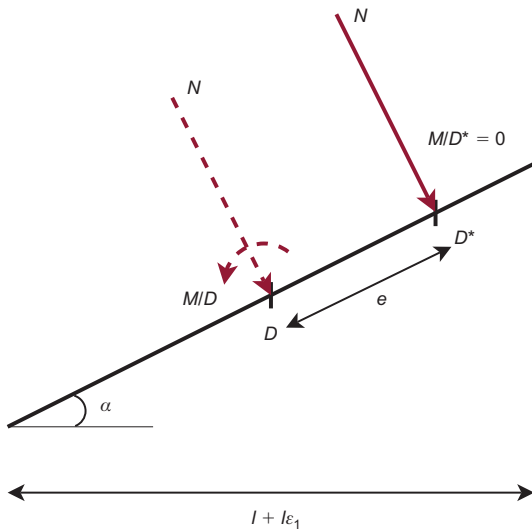
Fig. 7. Definition of wall eccentricity

Fig. 8. Profiles of walls V5s and C4L (thick lines: initial profile of walls before loading)

retain the cohesionless backfill and favour plain strain, which prevented the failure of the wall. This three-dimensional phenomenon is specific to large block walling. The trial will not be utilised.

Experiments show that drystone walls present two behaviours during loading; a global rotation around their toe, and a shearing combined with a local rotation of the bed joints situated at the lower third of the wall. The experiments also reveal the ultimate loading height that the wall can withstand.

This paper is intended to validate the yield design model on the data and the information provided by these two experimental programmes.

ANALYSIS OF EXPERIMENTAL DATA PROVIDED BY FULL-SCALE EXPERIMENTS

In this section, experimental data will be analysed towards a better understanding of drystone wall behaviour. The different hypotheses of the yield design simulation will also be compared with the experiments to test their validity. These hypotheses are summarised in Table 3.

Plane-strain analysis of wall

The yield design simulation was performed in two dimensions, and the wall was assumed to be sufficiently long to be considered as being under plane strain.

In the experimental programme, side effects were minimised by

(a) the length of the wall compared with its width and its height
(b) lubrication of the backfill formworks to ensure two-dimensional soil behaviour
(c) the lack of contact between the wall and the formworks (this was a problem for walls C1g and, to a lesser degree, C3s).

Comparing the wall displacements measured by stereophotogrammetric and sensor devices at different points on the front face makes it possible to evaluate the plane-strain behaviour of the wall (Villemus *et al.*, 2007; Colas *et al.*, 2010b). Fig. 8 shows that the difference between profiles did not exceed 2 cm on wall V5s and wall C4L, and thus validates the plane-strain hypothesis.
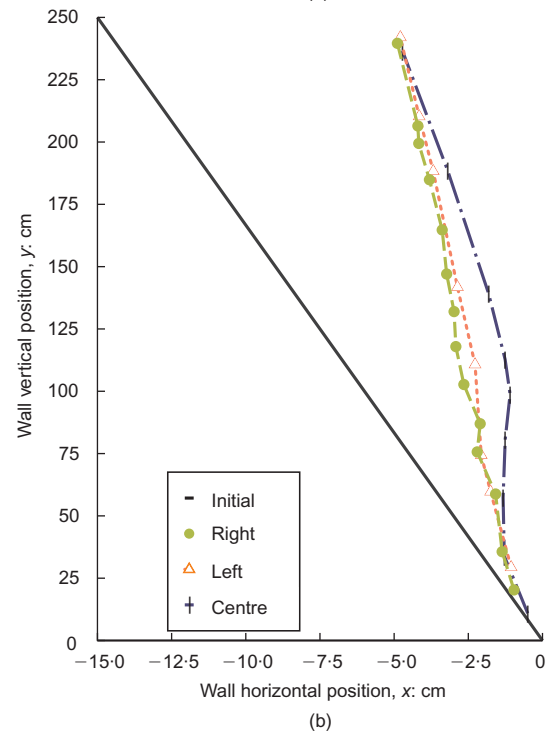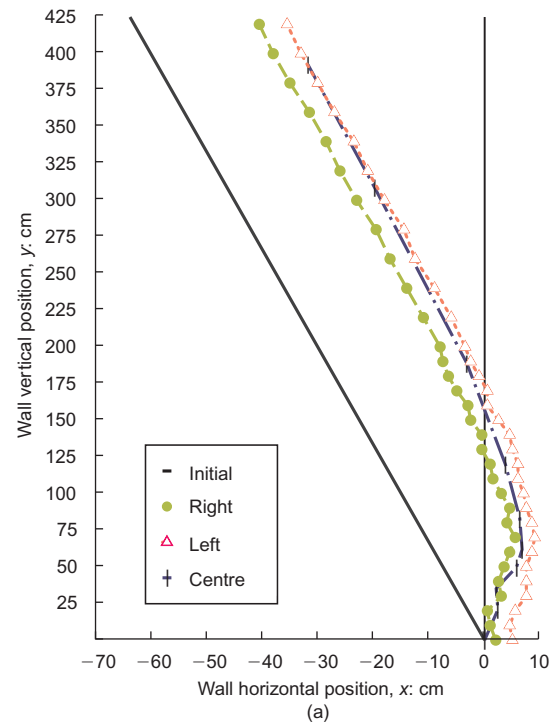
Regularity of blocks and masonry

For simulation purposes, drystone masonry was assumed to be composed of regular blocks of the same geometry that were fitted at regular (periodic) intervals. Drystone walls actually have certain regularities, but they are not purely periodic. Experiments have proven the important role of through stones in drystone wall stability (Dickens & Walker, 1996). On the other hand, the presence of a void enables a local rotation of the blocks at the basement, where loadings are the highest (Villemus *et al.*, 2007).

The presence of voids also influences the wall unit weight, which is different from the block unit weight. Yet the void percentage is extremely difficult to estimate, given the

Table 3. Summary of different hypotheses for drystone retaining structures characteristics

Parameters	Drystone walls	Simulation	Experiments
Dimension	3D/2D	2D	3D/2D
Masonry	Irregular	Regular	Irregular
Backfill	Unsaturated soil	Pulverulent soil	Pulverulent soil

heterogeneity of the wall. The experimental programmes described previously aimed to provide complementary information on this parameter. After each experiment, the stone blocks composing the wall were weighed to estimate the wall void percentage; the results are presented in Table 4.

The first four walls, which were built with the same limestone supply, have the same void percentage ($24{\cdot}8 \pm 1{\cdot}7\%$). This void percentage is far more significant than the void percentage of wall C4L, which was made with a different limestone supply. Similarly, the void percentage is greater in wall V5s than in walls C2s and C3s; walls C2s and C3s were made of the same schist, which was different from the schist used in wall V5s. Apart from differences in the stone, the void percentage may have been affected by the quality of the stone supply in the Villemus experiments; the limestone blocks were of poor quality, and there was a lack of pins in the schist supply. For practical use, the void percentage can be estimated at around 25% for walls composed of small blocks and around 15% for walls constructed with large blocks. If the supply of stone is poor, then this percentage can increase by up to 8 percentage points.

Periodic homogenisation

In the simulation, the masonry yield strength was determined by periodic homogenisation implemented within the field of yield design, where blocks are considered as infinitely resistant, and joints resort to a purely frictional Mohr–Coulomb criterion (see subsection 'Hypotheses' above).

During the experimentation, the maximal normal efforts recorded (around 150 kPa) were much lower than the compression strength of a pile of blocks measured in Villemus (2004) (around 800 kPa). This shows that the blocks can be considered as infinitely resistant.

For experimental walls backfilled with gravel, the wall slenderness ratio was low compared with existing walls designed with a factor of safety. Thus there were only one or two blocks in the wall thickness, which is not enough to validate the use of homogenisation (Fréard, 2000). The consistency of homogenisation will be proven by quantitative results (see the comparison section below).

Wall overturning

Experimental tests have shown that a drystone wall overturns around its toe when loaded with a hydrostatic pressure or a soil backfill. This phenomenon can be evaluated by the evolution of the wall angle of rotation, θ, as a function of the relative eccentricity, k (Fig. 9).

Figure 9 shows that all experimental angles of rotation have the same behaviour: a slow progression that can be considered to be linear at the beginning, and then a vertical asymptote. However, two specific behaviours can be identified, depending on the type of stone used in the wall (see lines for limestone and schist in Fig. 9). Only curve V3l

Table 4. Voids percentage of drystone experimental walls

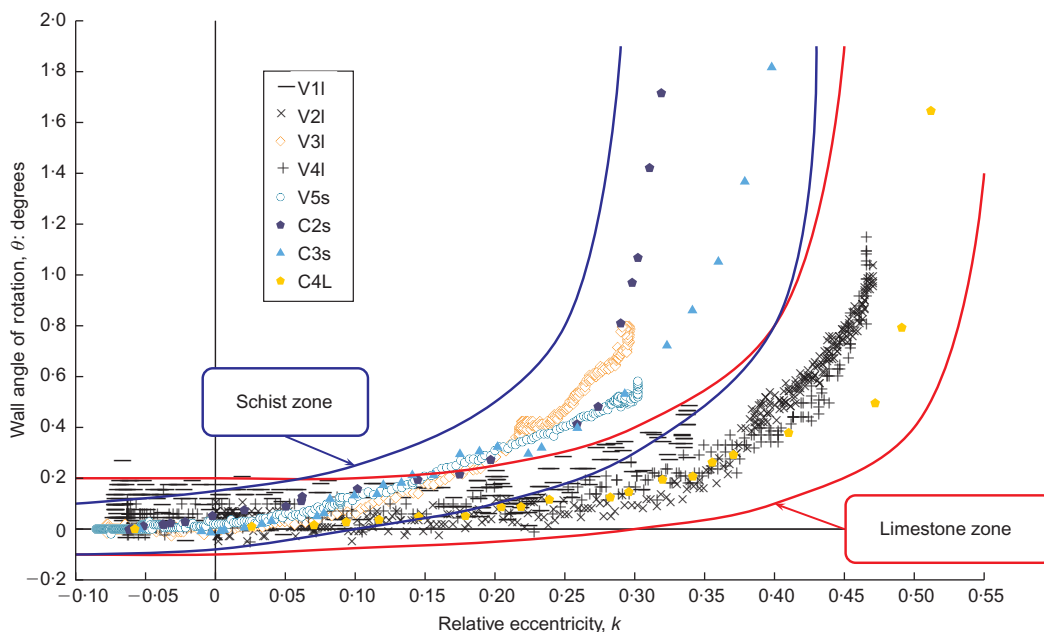|	V1l	V2l	V3l	V4l	V5s	C1g	C2s	C3s	C4L
Block unit weight: kN/m³	20·7	20·7	20·7	20·7	26·5	24·9	26·4	26·4	26·0
Voids percentage: %	25	27	24	23	32	16	24	24	16

Fig. 9. Overturning of experimental drystone walls: wall angle of rotation θ against relative eccentricity k

does not agree with this theory. During this experiment, the wall front face broke away, which resulted in an 'opening' of the wall (Fig. 10(a)). Two factors may account for this phenomenon: overcharge of the bearing capacity of the foundation, leading to foundation failure (Fig. 10(b)); compression failure of the pins used at the wall sides, resulting in spreading of the right-angle quoins (Fig. 10(c)).

In Fig. 9, it can also be seen that curves V1l, V2l and V4l are spread out, which can be attributed to the lack of accurate sensors during these experiments. Curves V1l, V3l and V5s seem truncated; this is due to the fact that these walls did not fail by overturning but by sliding (i.e. the wall rotation was not complete). In the same way, curves V2l and V4l were not fully completed, because these walls present both modes of failure. Hydrostatic pressure promotes shearing over overturning. The relative eccentricity, k, of wall C4L exceeds 0·5, which is theoretically impossible. Actually, the heterogeneity of the drystone structure allowed a rearrangement of the blocks composing the wall, which prevented the wall from overturning for $k < 0.5$. Considering the changes in the geometry of the wall, this relative eccentricity is just given as a rough guide.

Table 5 presents the ultimate overturning eccentricities and the corresponding loading heights and angles of rotation. The results for walls that did not completely overturn (walls V1l, V3l, V5s) are indicated in italics. Limestone walls failed at a relative eccentricity around 0·40. The ultimate eccentricity should be lower for schist walls, but was difficult to estimate, considering the uncertainties on wall C3s and the mixed shearing/overturning failure of wall C2s. The critical angle of rotation was quite low (approximately 0·5°), except for wall C3s, owing to the problem of friction on the formworks.

Wall shearing

Experiments have also shown that shearing occurred in the bed joints located at the lower third of the wall. Shearing is analysed using graphs of the ratio between tangential, T, and normal, N, forces acting on a bed joint depending on the relative displacement, $\delta u^{(i)}$, of the bed joint (Fig. 11).

Figure 11 shows curves similar to those from shear box tests on smooth blocks performed to design the wall (Villemus et al., 2007; Colas et al., 2010b): T/N increased steadily until it approached a horizontal asymptote. Two behaviours can also be identified, depending on the type of stone composing the wall. Although the schist and the limestone used in the two experimental programmes were different, they had very similar friction angles. Thus the authors infer that the shear behaviour is linked to the friction angle of the stone.

Curves V3l and V5s approach the horizontal asymptote, as they fail only by shearing, whereas the other walls fail also by overturning (see previous subsection). Asymptotes can be associated with a friction coefficient of the bed joints of the wall. The friction angle of the bed joints is roughly similar for the first four experiments ($\phi = 31.1 \pm 1.1°$), which were performed with the same limestone. The same is true for wall C2s and C3s, which were built with the same schist.

For each wall, the friction coefficient of the bed joints deduced from Fig. 11 can be compared with the friction coefficient of the blocks composing the wall measured through shear box testing (Table 6). This comparison shows that the values are very close; however, the bed joint friction angles are lower (difference around 7°) than the block friction angles measured by shear box tests. This could be due to local block rotation combined with global rotation of the wall, which favours sliding of the beds. In fact, the
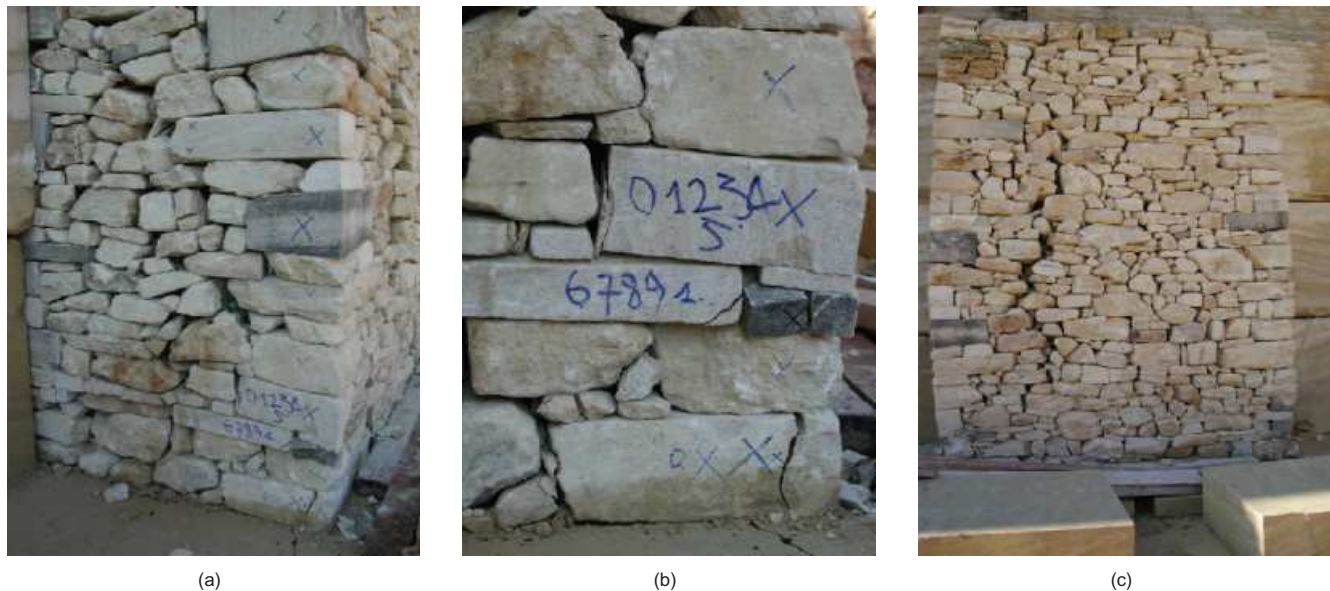

Fig. 10. (a) Wall V3l 'opening' due to (b) foundation failure, and (c) right-angle quoins spread

Table 5. Outcome of experimental drystone wall overturning

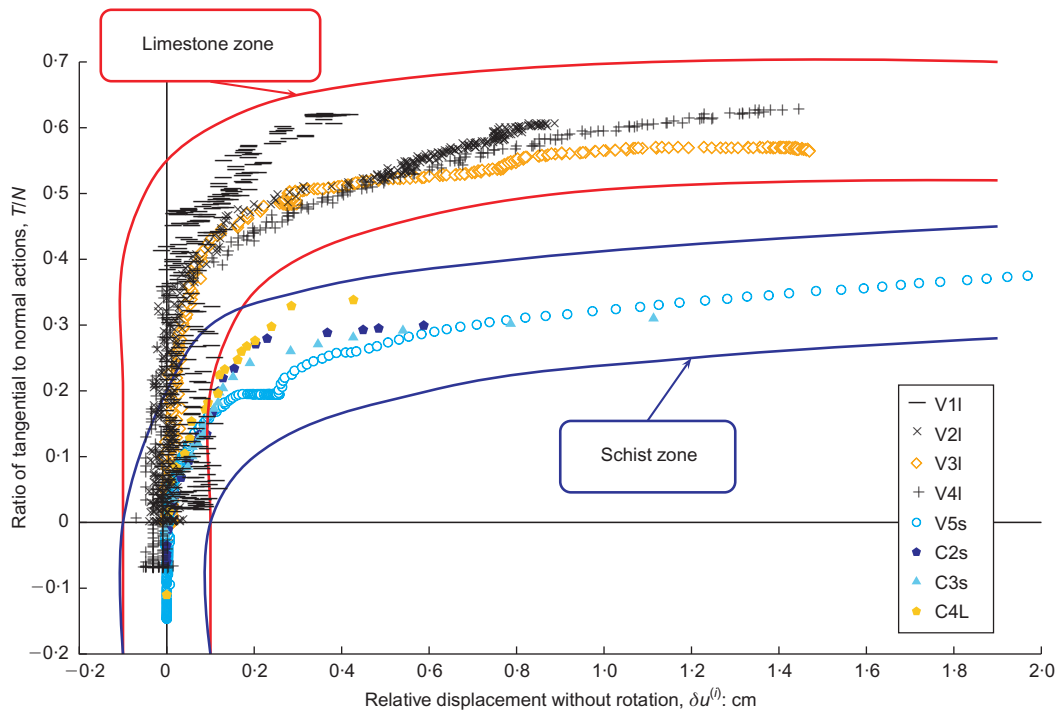|	V1l	V2l	V3l	V4l	V5s	C2s	C3s	C4L
Wall height: m	2·00	1·95	4·00	2·00	4·25	2·50	2·50	2·50
Critical loading height: m	1·74	1·78	3·37	1·90	3·62	2·30	2·78	2·72
Critical eccentricity	0·33	0·38	0·29	0·42	0·30	0·27	0·36	0·41
Critical angle of rotation: degrees	0·4	0·4	0·7	0·5	0·5	0·5	1·2	0·4
Overturning	Yes	Yes	No	Yes	No	Yes	Yes	Yes

Fig. 11. Shearing of experimental drystone walls: ratio of tangential/normal forces T/N on a bed joint against relative displacement $\delta u^{(i)}$

Table 6. Outcome of experimental drystone wall shearing

	V1l	V2l	V3l	V4l	V5s	C2s	C3s	C4L
Wall height: m	2·00	1·95	4·00	2·00	4·25	2·50	2·50	2·50
Shearing band: m	0·6	0·5	0·8	0·4	0·9	0·8	0·8	0·8
Critical loading height: m	1·72	1·90	3·36	1·94	3·61	2·34	2·96	2·95
Bed joint friction angle: degrees	31·1	31·0	29·7	32·2	23·2	16·7	> 17·7	> 19·2
Local rotation angle: degrees	*	*	*	*	*	2	2	3
Block friction angle: degrees	36·0	36·0	36·0	36·0	28·5	25·0	25·0	35·0
Shearing	Yes	Yes	Yes	Yes	Yes	Yes	No	No

* Local block rotation was not measured for these tests.

presence of voids in drystone masonry makes it possible for blocks to have a greater rotation than the wall. This local angle of rotation, Θ, is evaluated at around 2° by superposition of numerical photographs of the wall (Fig. 12). The remaining variation can be attributed to the difference in contact between the shear box block joints and the in situ bed joints.

COMPARISON BETWEEN THEORETICAL AND EXPERIMENTAL RESULTS

The final step of this work was to compare the theoretical, model-based predictions and the experimental results.

Definition of ultimate loading height

The yield design upper-bound theory used in the simulation provided an upper-bound limit to the ultimate loading height that the drystone wall could withstand. Two different heights are calculated here using equation (3); these heights correspond to the two failure mechanisms (sliding and overturning) tested in this simulation. The lower height was selected as stipulated by the yield design upper-bound approach. The difficulty was to set the physical parameters of the system, including the soil unit weight, γ_s, the soil

friction angle, ϕ_s, and the block friction angle ϕ. Uncertainties in the characterisation of mechanical parameters led to uncertainties in the ultimate loading height that was given by the simulation.

In a first attempt, the experimental ultimate loading height could be defined as the loading height that led to construction failure. However, as has been demonstrated earlier, the wall is subjected to either global overturning around its toe or shearing combined with local rotation of the blocks in the lower third of the wall, and for each failure mode a level indicating the mechanical failure of the wall can be identified. The authors decided to assimilate the experimental failure of the wall to the mechanical failure level recorded in Tables 5 and 6.

Experimental and theoretical results are recorded in Table 7. The analytical results are calculated using equation (3) for the two cases of possible kinematics described in Fig. 4 (overturning and sliding). The smallest value is the result (the fifth column of Table 7).

Comparison between theoretical and experimental ultimate loads

Each test should be studied carefully, considering the specificities of each experiment and the problems encoun-
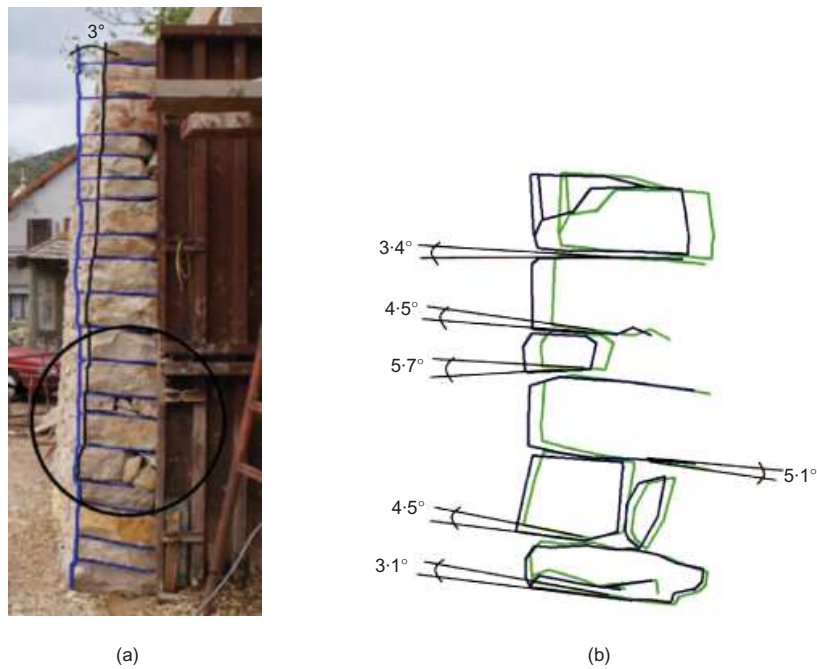
Fig. 12. Measurement of (a) global rotation of wall, θ, and (b) local rotation of blocks, Θ

Table 7. Comparison between theoretical and experimental ultimate backfill heights

Wall	Wall height: m	Exp. failure mode		Exp. load: m	Theor. load: m	Error: %
V1l	2·00	Sliding	Yes	1·74	1·86	6
		Overturning	No	–	1·92	
V2l	1·95	Sliding	Yes	1·90	1·98	4
		Overturning	Yes	1·78	1·92	
V3l	4·00	Sliding	Yes	3·37	3·74	11
		Overturning	No	–	3·86	
V4l	2·00	Sliding	Yes	1·94	2·00	2
		Overturning	Yes	1·90	1·94	
V5s	4·25	Sliding	Yes	3·60	3·98	10
		Overturning	No	–	4·11	
C2s	2·50	Sliding	Yes	2·30	3·18	12
		Overturning	Yes	2·30	2·58	
C3s	2·50	Sliding	No	–	4·19	3
		Overturning	Yes	2·78	2·85	
C4L	2·50	Sliding	No	–	6·46	2
		Overturning	Yes	2·72	2·67	

tered. For hydrostatic pressure experiments, sliding and overturning theoretical predictions were quite close (error less than 4%). Walls V2l and V4l experienced a combined sliding/overturning failure, whereas walls V1l, V3l and V5s experienced only a sliding failure, although they were close to overturning. Yield design succeeds in predicting the ultimate loading with an error of less than 11%; it also gives an indication of the type of failure. The most important error rate occurs when the wall failed solely by sliding. This may be due to the local rotation of the bed joints observed in the experiments, which is not assimilated in the model.

For walls loaded with a soil backfill, yield design provides a very high sliding ultimate height. However, experiments show that wall C2s failed by sliding and wall C3s was close to its sliding limit. Yield design seems to overestimate the sliding ultimate height; this can be attributed to the choice of failure mechanism in the model. In fact, the experiment proved that the wall did not remain monolithic when sliding, as assumed by the model; the blocks of the lower third of the wall went through combined shearing and local rotation. On the other hand, yield design predicts the ultimate backfill height with an error of less than 10%.

The analysis was performed by comparisons between the lower theoretical and experimental values. Fig. 13 shows the theoretical ultimate height plotted against the experimental ultimate height; the distance of each point to the first bisector gives an indication of the error rate. This shows the relevance of yield design for assessing drystone wall stability in two dimensions. Yield design succeeds in providing an estimate that is close to, and usually higher than, the experimental value, in accordance with the upper-bound approach used in the simulation. This also enables validation of the different hypotheses taken for the model, as well as the choice of the laboratory tests to characterise the constituent material of the wall and the backfill.

The uncertainties of the model can be appreciated in a first approach by evaluating the impact of a slight variation of each parameter on the prediction of the ultimate backfill
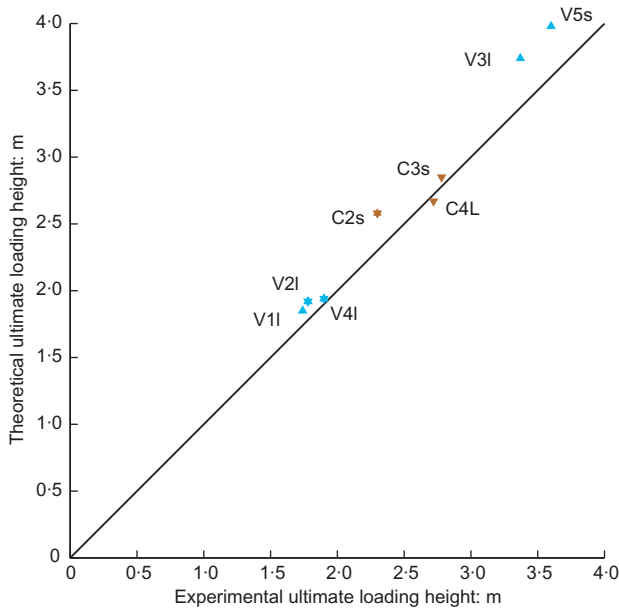
Fig. 13. Theoretical ultimate height against experimental ultimate height

height. As for geometric parameters, a variation of 1 cm or 1° has little influence on the model predictions (less than 5%). The influence of uncertainties is more obvious for mechanical parameters that are more difficult to obtain. Fig. 14 shows that if the ultimate backfill height is only slightly sensitive to variations of the wall unit weight, γ, or of the backfill unit weight, γ_s, then the friction angle of the blocks, ϕ, and more specifically that of the soil, ϕ_s, has a greater influence.

CONCLUSION

This paper aimed to analyse the behaviour of drystone retaining walls using yield design simulation and full-scale field trials. This work has highlighted or enhanced the understanding of the specific behaviours of drystone walls subjected to external loading. These specific behaviours include global overturning and sliding combined with local rotation of the blocks situated in the lower third of the wall. The results have also shown that the simulation succeeded in predicting the ultimate loading that a drystone wall can withstand, with an error rate of approximately 10%. The simulation provided complementary information on the type of failure of the wall. The simulations enable validation of the hypotheses of the model, which is related to the periodicity of the masonry and the failure modes. Finally, the results reinforce the use of the tests chosen to characterise the constituent materials of the wall and the backfill, as well as the soil–structure interaction described in Colas *et al.* (2010b).

This study has also revealed some limitations of the model, which is less well suited to predicting sliding failure. It could be interesting to experiment with new failure mechanisms, because of the mixed local sliding–rotating process that was observed experimentally. This limit could also be due to the hypothesis of a periodic medium. It would be interesting to explore the field of random media. Further perspectives on this work could also take into account new loadings, such as overloading the backfill or seismic conditions. Finally, this work may lead to the diagnosis of existing walls. The rich drystone heritage, dating mainly from the nineteenth century, shows significant pathologies, and notably bulging deformations, which must be evaluated and/or repaired.
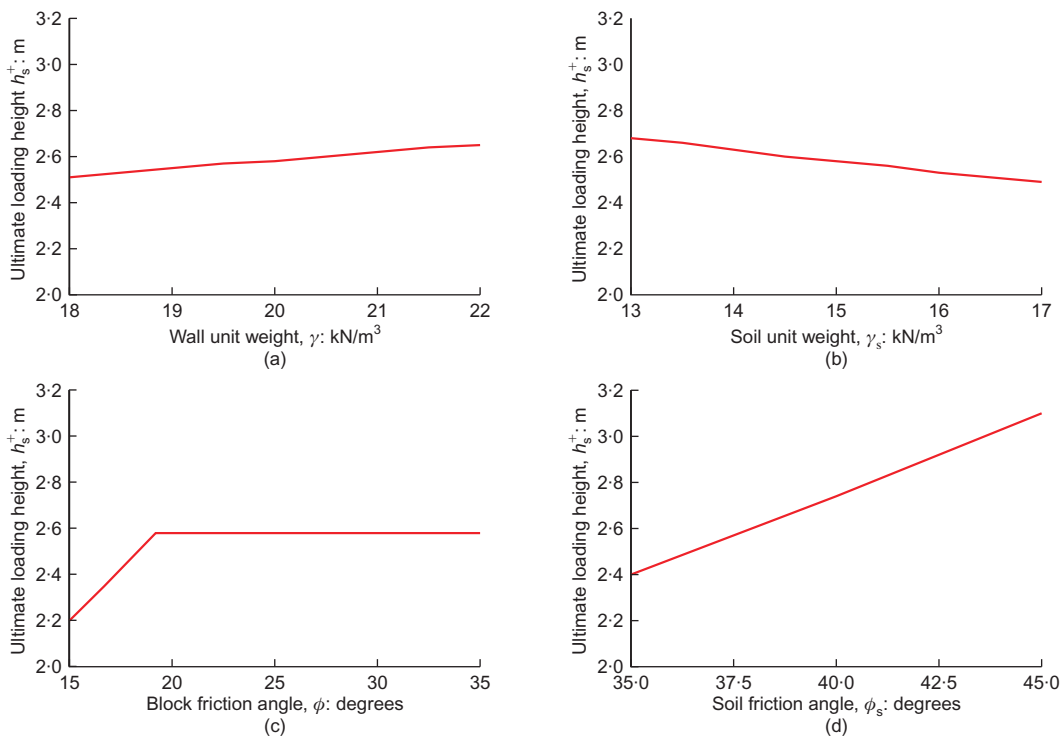
Fig. 14. Influence of parametric variations on ultimate loading height: (a) wall unit weight; (b) soil unit weight; (c) block friction angle; (d) soil friction angle

NOTATION

D	centre of foundation
D^*	application point of centric force
e	wall eccentricity
f	notation of $\tan\phi$
f_1	wall batter
f_2	wall counterslope
h	height of wall
h_1	loading height
h_s	backfill height
h_s^+	ultimate loading height
k	wall relative eccentricity
L	length of wall
l	thickness at top of wall
m	slenderness ratio of blocks
N	normal force acting on bed joint
p_0, p_1, p_2, p_3	coefficients of the cubic function
T	tangential force acting on bed joint
v	virtual velocity field
v_m	virtual velocity field in the wall
v_s	virtual velocity field in the soil
W^e	work of external forces
W^{mr}	maximum resisting work
x	wall horizontal position
y	wall vertical position
α	joint inclination
β	backfill slope
γ	unit weight of wall
γ_s	unit weight of backfill
δ	interface friction angle
$\delta u^{(i)}$	relative displacement of bed joint
Θ	local angle of rotation
θ	wall angle of rotation
λ_1	front batter of wall
λ_2	back batter of wall
Σ	principal homogenised stress tensor
ϕ	block friction angle
ϕ_s	soil friction angle

REFERENCES

Arya, A. S. & Gupta, V. P. (1983). Retaining walls for hill roads. *Indian Roads Congress J.* **44**, No. 1–4, 291–326.

de Buhan, P. & de Felice, G. (1997). A homogenization approach to the ultimate strength of brick masonry. *J. Mech. Phys. Solids* **45**, No. 7, 1085–1104.

Claxton, M., Hart, R. A., McCombie, P. F. & Walker, P. J. (2005). Rigid block distinct-element modeling of dry-stone retaining walls in plane strain. *J. Geotech. Geoenviron. Engng* **131**, No. 3, 381–389.

Colas, A. S. (2009). *Mécanique des murs de soutènement en pierre sèche: modélisation par le calcul à la rupture et expérimenta-tion échelle 1*. PhD thesis, ENTPE–ECL, Vaulx-en-Velin, France (in French).

Colas, A. S., Morel, J. C. & Garnier, D. (2008). Yield design of dry-stone masonry retaining structures: Comparisons with analytical, numerical, and experimental data. *Int. J. Numer. Anal. Methods Geomech.* **32**, No. 14, 1817–1832.

Colas, A. S., Morel, J. C. & Garnier, D. (2010a). 2D modelling of a dry joint masonry wall retaining a pulverulent backfill. *Int. J. Numer. Anal. Methods Geomech.* **34**, No. 12, 1237–1249.

Colas, A. S., Morel, J. C. & Garnier, D. (2010b). Full-scale field trials to assess dry-stone retaining wall stability. *Engng Struct.* **32**, No. 5, 1215–1222.

Cooper, M. R. (1986). Deflections and failure modes in dry-stone retaining walls. *Ground Engng* **19**, No. 8, 40–45.

Dickens, J. G. & Walker, P. J. (1996). Use of distinct element model to simulate behaviour of dry-stone walls. *Struct. Engng Rev.* **8**, No. 2–3, 187–199.

Fréard, J. (2000). *Analyse de la stabilité des massifs rocheux fracturés par une méthode d'homogénéisation*. PhD thesis, ENPC, Marne-la-Vallée, France (in French).

Harkness, R. M., Powrie, W., Zhang, X., Brady, K. C. & O'Reilly, M. P. (2000). Numerical modelling of full-scale tests on dry-stone masonry retaining walls. *Géotechnique* **50**, No. 2, 165–179, http://dx.doi.org/10.1680/geot.2000.50.2.165.

Mundell, C., McCombie, P. F., Bailey, C., Heath, A., & Walker, P. (2009). Limit equilibrium assessment of drystone retaining structures. *Proc. Inst. Civ. Engrs Geotech. Engng* **162**, No. 4, 203–212.

Mundell, C., McCombie, P., Heath, A., Harkness, J. & Walker, P. (2010). Behaviour of drystone retaining structures. *Proc. Instn Civ. Engrs Struct. Build.* **163**, No. 1, 3–12.

O'Reilly, M. P., Bush, D. I., Brady, K. C. & Powrie, W. (1999). The stability of drystone retaining walls on highways. *Proc. Instn Civ. Engrs Municip. Engr* **133**, No. 2, 101–107.

Odent, N. (2000). Recensement des ouvrages de soutènement en bordure du réseau routier national. *Bull. Ouvrages d'Art* **34**, 15–18.

Powrie, W., Harkness, R. M., Zhang, X. & Bush, D. I. (2002). Deformation and failure modes of drystone retaining walls. *Géotechnique* **52**, No. 6, 435–446, http://dx.doi.org/10.1680/geot.2002.52.6.435.

Salençon, J. (1990). An introduction to the yield design theory and its application to soils mechanics. *Eur. J. Mech. A Solids* **9**, No. 5, 477–500.

Villemus, B. (2004). *Étude des murs de soutènement en maçonnerie de pierres sèches*. PhD thesis, ENTPE–INSA de Lyon, France (in French).

Villemus, B., Morel, J. C. & Boutin, C. (2007). Experimental assessment of dry stone retaining wall stability on a rigid foundation. *Engng Struct.* **29**, No. 9, 2124–2132.

Zhang, X., Koutsabeloulis, N. C., Hope, S. & Pearce, A. (2004). A finite element analysis for the stability of drystone masonry retaining walls. *Géotechnique* **54**, No. 1, 57–60, http://dx.doi.org/10.1680/geot.2004.54.1.57.